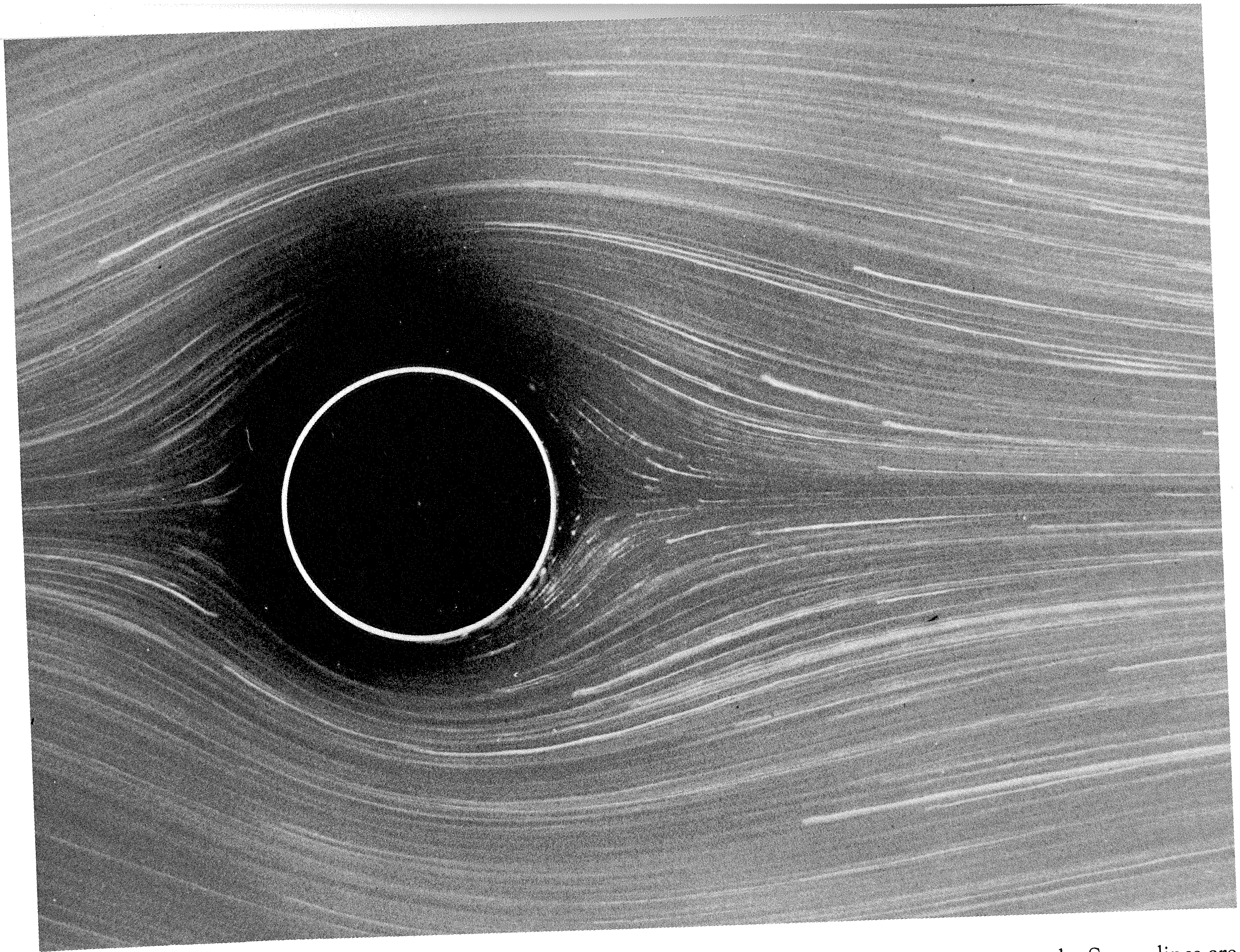

24. Circular cylinder at R=1.54. At this Reynolds number the streamline pattern has clearly lost the fore-and-aft symmetry of figure 6. However, the flow has not yet separated at the rear. That begins at about R=5, though the value is not known accurately. Streamlines are made visible by aluminum powder in water. *Photograph by Sadatoshi Taneda*

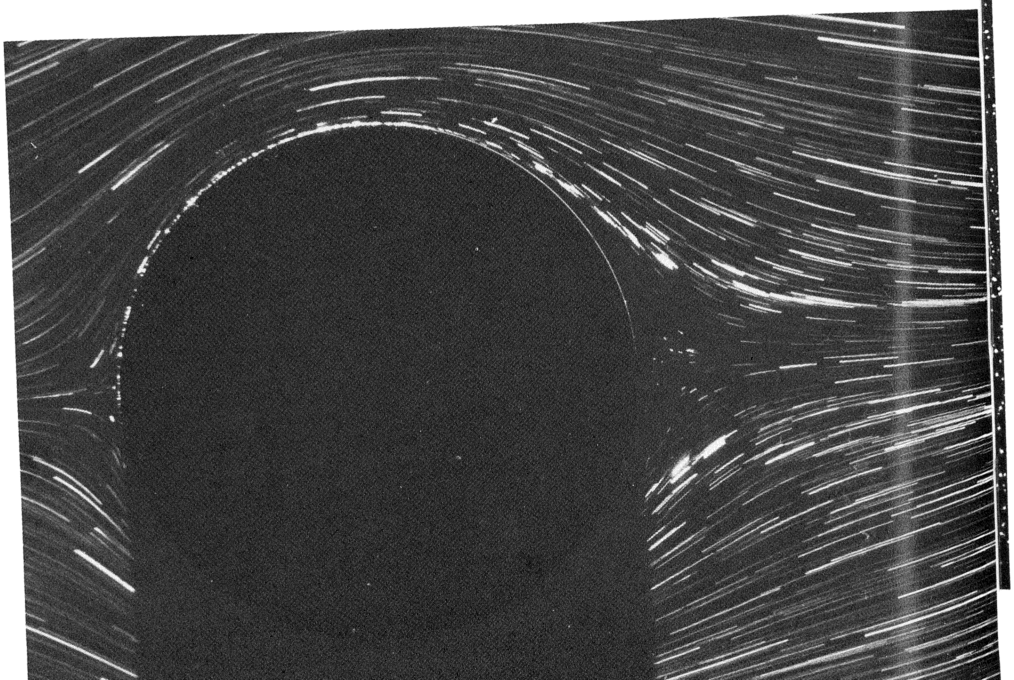

25. Sphere at R=9.8. Here too, with wall effects negligible, the streamline pattern is distinctly asymmetric, in contrast to the creeping flow of figure 8. The fluid is evidently moving very slowly at the rear, making it difficult to estimate the onset of separation. The flow is presumably attached here, because separation is believed to begin above R=20. Streamlines are shown by magnesium cuttings illuminated in water. *Photograph by Madeleine Coutanceau and Michele Payard*

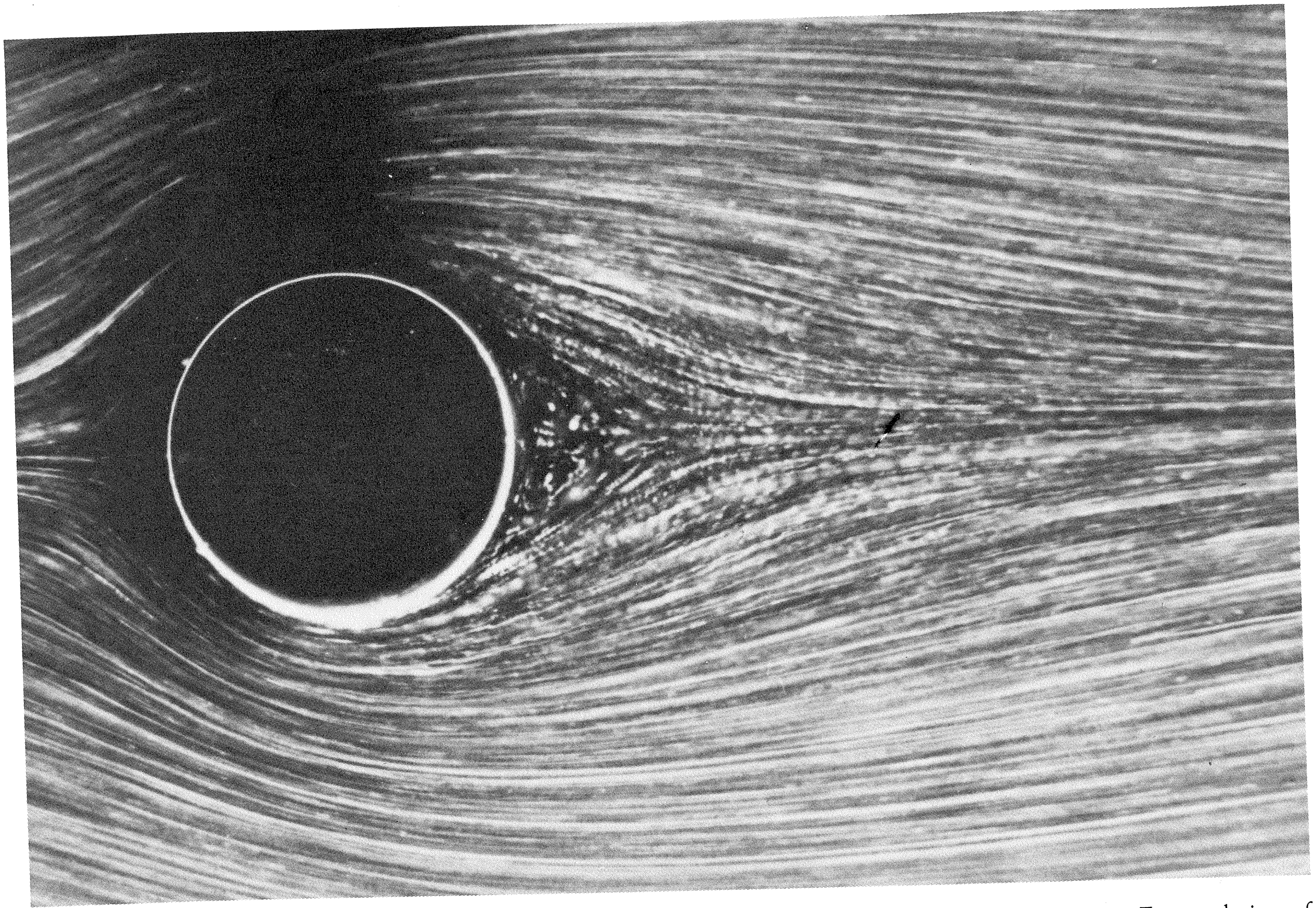

40. Circular cylinder at R=9.6. Here, in contrast to figure 24, the flow has clearly separated to form a pair of recirculating eddies. The cylinder is moving through a tank of water containing aluminum powder, and is illuminated by a sheet of light below the free surface. Extrapolation of such experiments to unbounded flow suggests separation at R=4 or 5, whereas most numerical computations give R=5 to 7. *Photograph by Sadatoshi Taneda*

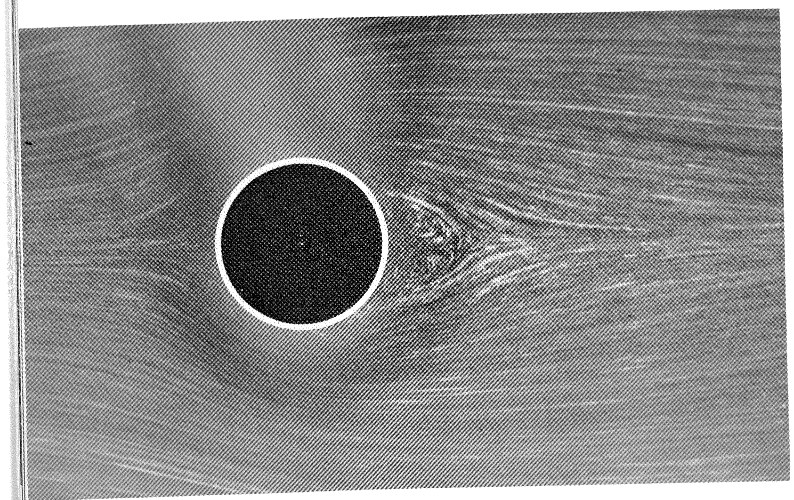

41. Circular cylinder at R=13.1. The standing eddies become elongated in the flow direction as the speed increases. Their length is found to increase linearly with Reynolds number until the flow becomes unstable above R=40. *Taneda 1956a*

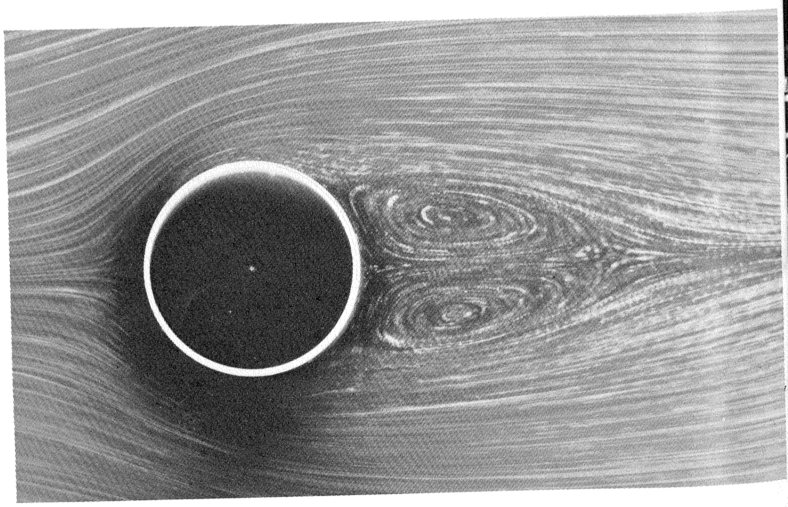

42. Circular cylinder at R=26. The downstream distance to the cores of the eddies also increases linearly with Reynolds number. However, the lateral distance between the cores appears to grow more nearly as the square root. *Photograph by Sadatoshi Taneda*

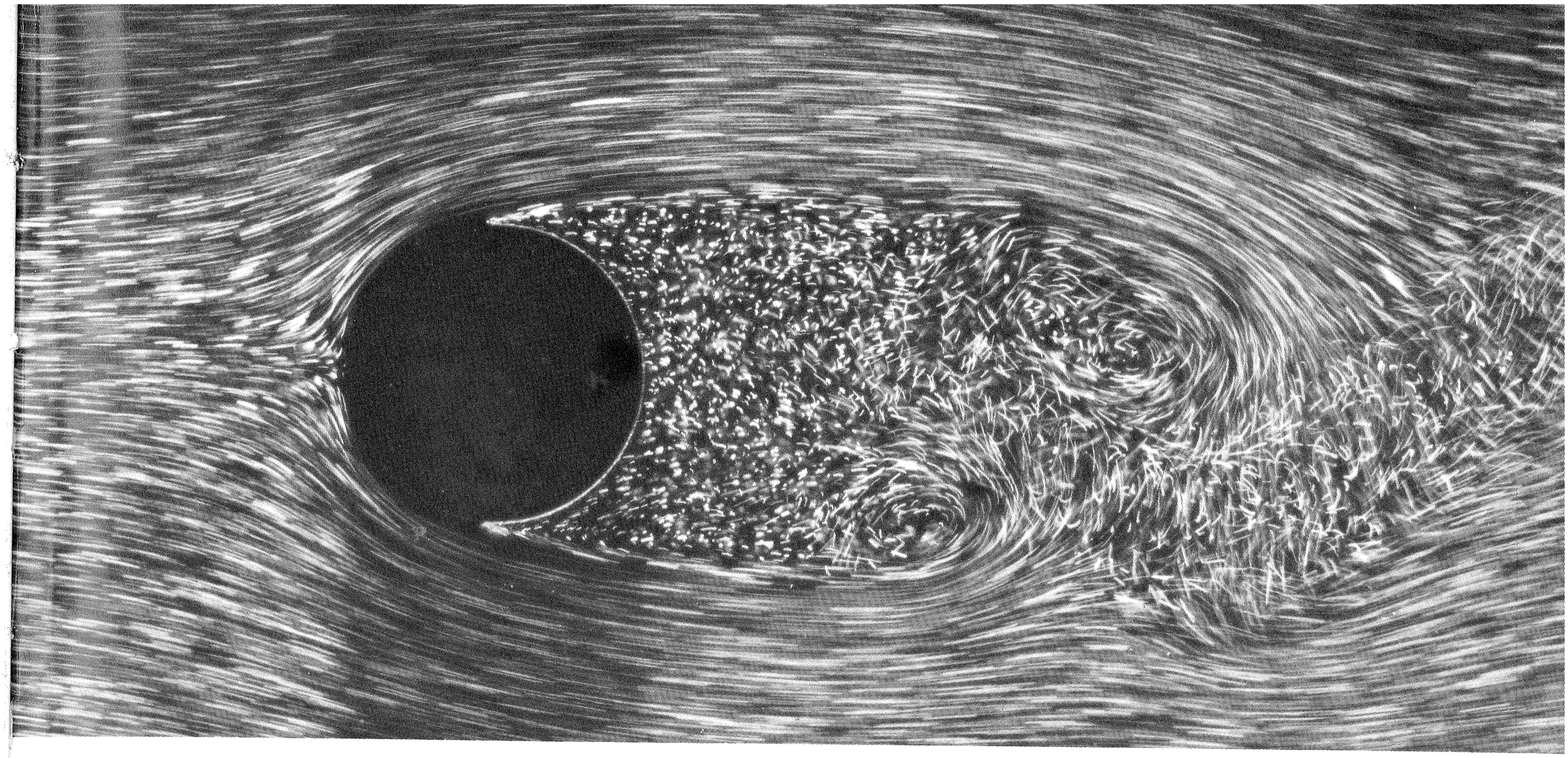

47. Circular cylinder at $R=2000$**.** At this Reynolds number one may properly speak of a boundary layer. It is laminar over the front, separates, and breaks up into a turbulent wake. The separation points, moving forward as the Reynolds number is increased, have now attained their upstream limit, ahead of maximum thickness. Visualization is by air bubbles in water. *ONERA photograph, Werlé & Gallon 1972*

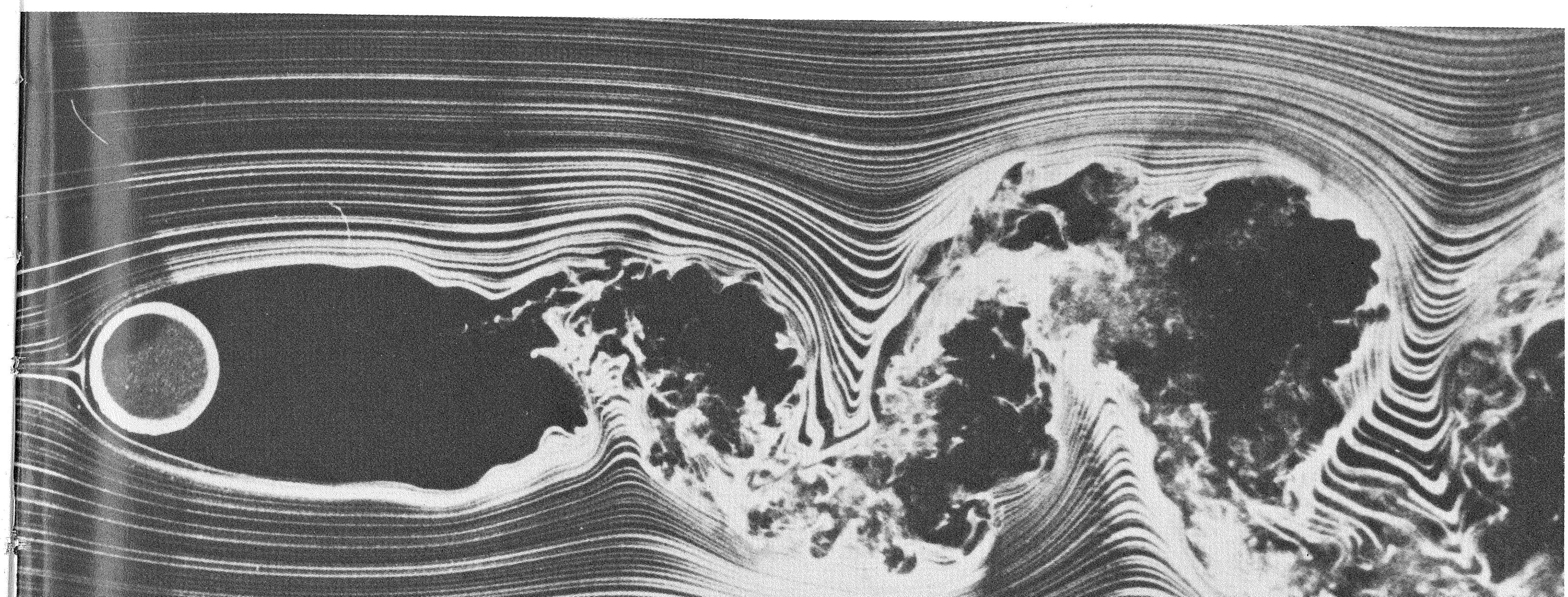

48. Circular cylinder at $R=10{,}000$**.** At five times the speed of the photograph at the top of the page, the flow pattern is scarcely changed. The drag coefficient consequently remains almost constant in the range of Reynolds number spanned by these two photographs. It drops later when, as in figure 57, the boundary layer becomes turbulent at separation. *Photograph by Thomas Corke and Hassan Nagib*

33. Boundary-layer separation on a body of revolution. This shape is sufficiently blunter than the Rankine ogive of figure 22 that, at the same Reynolds number of 6000 based on diameter and zero incidence, the laminar boundary layer separates. It then quickly becomes turbulent and reattaches to the surface, enclosing a short thin region of recirculating flow. Visualization is by air bubbles in water. *ONERA photograph, Werlé 1962*

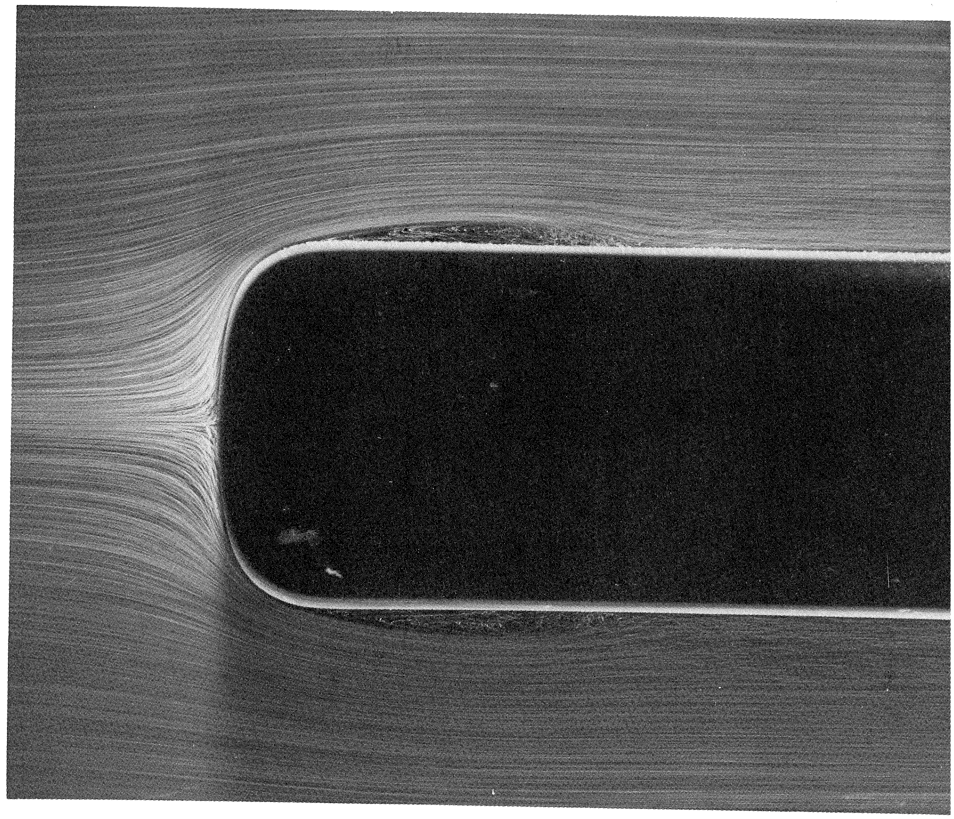

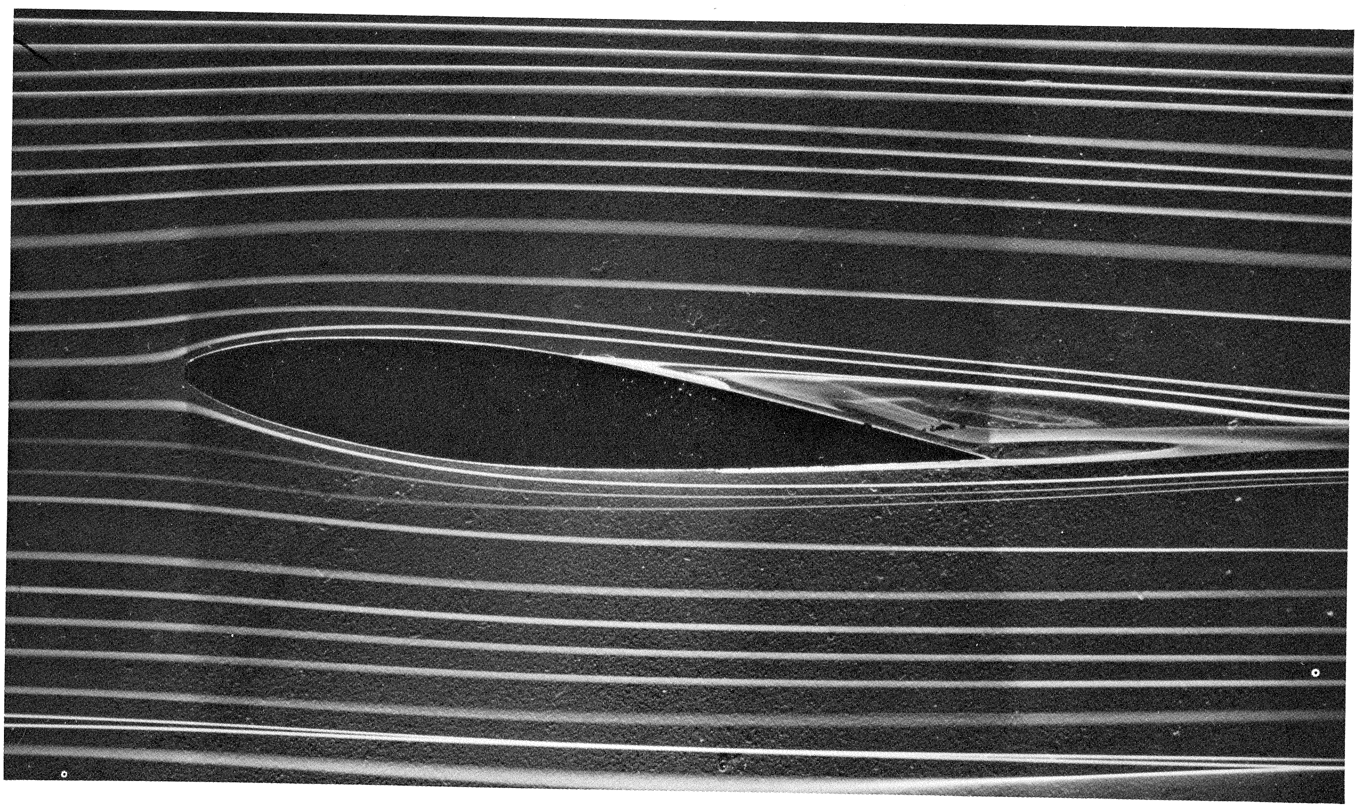

34. Boundary-layer separation on an inclined airfoil. When the NACA 64A015 airfoil of figure 23 is raised to 5° incidence the laminar boundary layer separates from the rear half of the upper surface. The flow remains attached to the lower surface, from which it leaves tangentially at the trailing edge. Streamlines are shown by colored fluid filaments in water. *ONERA photograph, Werlé 1974*